Insights into COVID-19 epidemiology and control from temporal changes in serial interval distributions in Hong Kong

Sheikh Taslim Ali[1,2,†], Dongxuan Chen[1,2,†], Wey Wen Lim[1,2], Amy Yeung[1,2], Dillon C. Adam[1,2], Yiu Chung Lau[1,2], Eric H. Y. Lau[1,2], Jessica Y. Wong[1], Jingyi Xiao[1], Faith Ho[1], Huizhi Gao[1], Lin Wang[3], Xiao-Ke Xu[4], Zhanwei Du[1,2], Peng Wu[1,2], Gabriel M. Leung[1,2,‡], Benjamin J. Cowling[1,2,‡]

Affiliations:

[1] WHO Collaborating Centre for Infectious Disease Epidemiology and Control, School of Public Health, Li Ka Shing Faculty of Medicine, The University of Hong Kong, Hong Kong Special Administrative Region, China

[2] Laboratory of Data Discovery for Health Limited, Hong Kong Science and Technology Park, New Territories, Hong Kong.

[3] Department of Genetics, University of Cambridge, Cambridge, United Kingdom,

[4] College of Information and Communication Engineering, Dalian Minzu University, Dalian 116600, China.

[†]These authors contributed equally to this work.

[‡]Joint senior authors

Corresponding author: bcowling@hku.hk

Abstract:

The serial interval distribution is used to approximate the generation time distribution, an essential parameter to predict the effective reproductive number "R_t", a measure of transmissibility. However, serial interval distributions may change as an epidemic progresses rather than remaining constant. Here we show that serial intervals in Hong Kong varied over time, closely associated with the temporal variation in COVID-19 case profiles and public health and social measures that were implemented in response to surges in community transmission. Quantification of the variation over time in serial intervals led to improved estimation of R_t, and provided additional insights into the impact of public health measures on transmission of infections.

One-Sentence Summary:

Real-time estimates of serial interval distributions can improve assessment of COVID-19 transmission dynamics and control.

Main Text:

Monitoring the intensity of coronavirus disease 2019 (COVID-19) transmission is an essential component of public health surveillance for situational awareness and real-time impact assessment of interventions (*1, 2*). Transmissibility has typically been measured by the effective reproductive number "R_t" based on analysis of epidemic curves along with an estimate of the generation time distribution (*3-5*). The generation time for an infectious disease describes the average time between consecutive infections in a transmission chain (*4, 6*), and is often approximated by the serial interval distribution which describes the average time between illness onsets of consecutive cases in a transmission chain (*3, 7, 8*). However, we and others have shown that the serial interval distribution may change as an epidemic progresses rather than remaining constant (*9-11*).

In Hong Kong, a subtropical city located on the southern coast of China, the public health responses to COVID-19 following a "dynamic zero covid" strategy aiming to eliminate local infections included a number of key components. First, travel restrictions and on-arrival quarantines on all in-bound travellers have been implemented throughout the pandemic to reduce the importation risk. Second, a series of targeted and community-wide public health and social measures have been used to minimize local transmission of COVID-19, including hospital isolation of all confirmed cases, quarantine of close contacts in designated facilities, mask mandate, restriction on gatherings, closures of facilities, schools, and some workplaces, and compulsory testing orders for persons at a higher risk of exposure. This strategy was successful in limiting cumulative incidence to 12,600 confirmed cases by 31 December 2021, corresponding to 0.16% of the total population in Hong Kong. All community epidemics were associated with ancestral-like viruses and not variants. Here, our objective is to take advantage of detailed contact tracing data in Hong Kong to characterise temporal changes within and

between waves in the serial interval distribution of COVID-19 through a series of community epidemics, and identify possible factors associated with those temporal changes.

COVID-19 transmission and PHSMs in Hong Kong

We obtained detailed information on each laboratory-confirmed case of COVID-19 from the Department of Health of the Hong Kong SAR government (section 1, supplementary materials). The database included information on the confirmation date, illness onset date, isolation date, hospital admission date, outcome (critical/serious/stable), infection origin (locally infected vs infected outside Hong Kong) and arrival date (if applicable), home and workplace location, detailed travel/movement history, cluster information from contact tracing (if applicable) of each confirmed case (*12*). In Hong Kong from 22 January 2020 through 31 July 2022, COVID-19 has caused five local epidemic waves. The "first wave", defined as the period from late January to mid-February 2020 with a small number of community cases linked to importations from mainland China (*13*). Given the very small number of imported infections (n=45) we excluded the first wave from our study. We analysed data from throughout the second wave (1 March 2020 – 10 April 2020), third wave (25 June 2020 – 8 September 2020) and fourth wave (1 Nov 2020 – 23 March 2021) (**Fig. 1A**). In the fifth wave which started in early January 2022 (*14*), contact tracing capacity was challenged due to the fast exponential rise in cases, and we were only able to include detailed data on confirmed transmission pairs from the very early stage of this wave in these analyses. Our study received ethical approval from the Institutional Review Board of the University of Hong Kong (ref: UW 20-341).

We collected information from official reports on the public health and social measures (PHSMs) implemented in Hong Kong to control the spread of COVID-19 (*15*). We further

101 classified these interventions into case-based, community-wide (including travel-based)
102 control measures (*16*). The case-based measures including strict isolation of cases and
103 quarantine of close contacts were maintained throughout each wave while the community-wide
104 measures were generally only implemented when needed to bring each epidemic wave under
105 control. The summary of these PHSMs including their timing and duration is provided in
106 Supplementary table S1.
107
108 **Construction of transmission pairs**
109 Following our earlier work (*17*), we first reconstructed the initial transmission pairs with
110 reference to the detailed individual data on all confirmed cases retrieved from the Centre for
111 Health Protection. We further rechecked the initially constructed pairs by their cluster
112 information and epidemiological linkage with other cases and determined the infector and
113 infectee within a pair according to a pre-defined algorithm (section 1, supplementary
114 materials). The larger clusters with complex epidemiological linkages between the cases were
115 individually assessed to determine the infector and the infectee in each transmission pair. If
116 there were two or more likely infectors in one cluster, we defined the infector as the case with
117 the earliest onset date. If cases shared the same onset date, the one with an earlier report date
118 or case number would be classified as an infector (section 1, supplementary materials) (*9, 18*).
119 We also performed a possible cross-check on unclear pairs with phylogenetic data to examine
120 potential infector-infectee relationships with the *Phybreak* package in R (*19*). We resolved the
121 multiple infector issue by identifying a case to be the infector of all subsequent cases with an
122 immediate link in a cluster when the onset intervals between the infector and the infectees fell
123 within a pre-defined time period, 8 days for the main analysis and 5-14 days for the sensitivity
124 analyses (section 6, supplementary materials). Among more than 12,600 COVID-19 cases in
125 Hong Kong in the period 1 March 2020 through to 23 March 2021, most were identified in the

126 third and fourth waves (**Fig. 1A**), in total we were able to construct 2433 transmission pairs,
127 including 87, 965 and 1381 in the second, third and fourth waves, respectively. Among these,
128 we considered 47, 357 and 355 transmission pairs as "confirmed pairs" in these three waves,
129 respectively, and the remainder were "likely pairs" (section 1, supplementary materials). There
130 were an additional 64 pairs identified in small outbreaks occurred between our pre-defined
131 waves, and 229 pairs (30 for BA1, 174 for BA2 and 25 for delta) identified in the very early
132 stage of the fifth wave (fig. S1).
133
134 **Time-varying serial intervals and PHSMs**
135 We estimated the serial interval distributions over time in a Bayesian framework based on
136 Markov Chain Monte Carlo, implemented with the *RStan* package in R (section 2,
137 supplementary materials). We estimated serial interval distributions for three periods within
138 each wave i.e. pre-peak, during peak, and post-peak, and then estimated the time-varying daily
139 effective serial interval distributions with a sliding window of 10 days (7-14 days for sensitivity
140 analysis) (*9*). We used the same framework to estimate the distributions of onset-to-isolation
141 intervals (indicating case isolation delay) for the infectors and then performed multivariable
142 regression analysis on mean serial intervals where the mean onset-to-isolation interval and
143 various PHSMs were included as explanatory variables (section 3, supplementary materials).
144 The variation in population mobility and mixing, potentially reflecting the effect of these
145 PHSMs, might also impact the transmission dynamics of COVID-19 (*20-22*). Therefore, we
146 also performed a multivariable regression analysis on the estimated mean serial intervals with
147 the daily digital transactions through Octopus cards, a widely-used contactless electronic
148 payment system in Hong Kong, as the proxy of relative mobility of the population (*20*), and
149 daily per capita testing volume (number of PCR tests conducted per 10,000 population per day)
150 in Hong Kong (section 3, supplementary materials).

Among the 2497 transmission pairs identified in during the first two years of the COVID-19 pandemic in Hong Kong including the second, third and fourth waves with the ancestral strain of SARS-CoV-2, the mean serial interval (μ) was estimated to be 3.6 (95% CrI: 3.5, 3.7) days with standard deviation (σ) 3.4 (95% CrI: 3.3, 3.5) days.

We identified the peak of the second wave from 16 to 24 March 2020, from 18 to 27 July 2020 for the third wave, and the fourth wave had two peaks, the first from 30 November 2020 to 15 December 2020 and the second during 11 - 25 January 2021 (section 1, supplementary materials). There were clear temporal changes in mean serial interval estimates within each epidemic wave studied and across waves, with mean serial intervals shortening from 5.5 days (95% CrI: 4.4, 6.6) for pre-peak to 3.2 days (95% CrI: 1.9, 4.4) for post-peak in the second wave, and from 4.6 (95% CrI: 4.1, 5.0) days to 2.7 (95% CrI: 2.2, 3.2) days in the third wave (**Fig. 1A** and table S2). However, less clear changes were identified in the fourth wave where two peaks in incidence were noted (**Fig. 1A**). The standard deviations of serial interval distributions within individual epidemic waves were more comparable but inter-wave differences were noticeable ranging from 2.4 days to 4.3 days (table S2). The mean onset-to-isolation intervals had a similar decreasing temporal pattern along with mean serial intervals during the second wave shortening from 5.8 days to 3.5 days, while the estimates were largely constant during the third wave between 5.2 days and 5.4 days and fluctuated throughout the fourth wave (3.4 days to 5.0 days) (**Fig. 1A** and table S2). In the early part of the fifth wave, the mean serial interval was estimated to be 3.6 (95% CrI: 3.5, 3.7) days with standard deviation 3.4 (95% CrI: 3.3, 3.5) days with comparable estimates for the Delta variant (μ: 4.0 days, σ: 2.4 days), the Omicron BA.1 (μ: 3.3 days, σ: 2.0 days) and the Omicron BA.2 (μ: 3.6 days, σ: 1.8 days) subvariants.

The time-varying mean effective serial intervals and onset-to-isolation intervals across the second, third and fourth epidemic waves in Hong Kong showed similar temporal patterns in the two epidemiological parameters based on the daily changes in the estimates (**Fig. 1, B to D**). The daily variations (shortening and lengthening) in the estimates of two parameters either occurred towards the same direction (most of the second wave, some phases of the third and the fourth waves) or opposite directions (some of the phases in the third wave and the fourth wave) over the epidemics. Similar results were also indicated in the sensitivity analysis on all transmission pairs (fig. S2).

The implemented PHSMs could explain up to 70%, 42% and 49% of the variance in the mean effective serial intervals estimated for the second, third and fourth waves, respectively (table S3). The onset-to-isolation interval, reflecting the impact of the targeted measure of case identification and isolation, was found to have statistically significant positive associations with the effective serial intervals for the second and third waves with up to 60% and 13% of the variations explained in the estimated effective serial intervals for the two waves respectively, but there was not a statistically significant association in the fourth wave. The interrupted regression further suggested similar associations between onset-to-isolation intervals and effective serial intervals during different phases of the epidemics (table S4). A maximum of 10%, 29% and 48% of the variances in the estimated serial intervals were explained in the three waves respectively by both types of PHSMs (community-wide and case-based measures) when adjusting for the possible delays in the impact of onset-to-isolation. The relative population mobility and daily tests per capita showed a positive and a negative association, respectively, with the mean effective serial interval across the waves (figs. S7 to S9 and table S5).

201

202 **Factor-specific effective serial intervals**

203 We also explored the association between the estimated serial intervals and characteristics of
204 the infector in the identified transmission pairs in the second, third and fourth wave, including
205 age, sex, source of infection, transmission setting, severity outcomes and onset-to-isolation
206 delay (section 4, supplementary materials). The mean serial interval estimates ranged from 2.4
207 days to 5.6 days across the strata of these characteristic factors for infectors (tables S6 and S7,
208 and fig. S3). We found that an older age (≥ 65 years) of the infectors was associated with a
209 higher estimate of the mean serial interval (p-value <0.023) across the waves (fig. S3A and
210 tables S7). The age-specific transmission matrices indicated that a higher proportion of the
211 secondary infections transmitted to younger (<35 years) infectees from the infectors of all age-
212 groups (**Fig. 2, A to C**) and initially (during pre-peak) infections started with older (>65 years)
213 infector-infectee transmissions, then involved more younger population during peak and post-
214 peak periods of the third and fourth waves (fig. S4). The age specific mean serial intervals were
215 longer for older infectors (e.g., ≥ 65 years) (**Fig 2, D to F** and fig. S5).

216

217 In the second wave, transmission setting was identified as a statistically significant explanatory
218 factor (p-value = 0.037) with a higher estimated mean serial interval for household transmission
219 (tables S6 and S7). In general, the estimates of mean serial intervals were longer for the
220 transmission pairs with critical/severe infectors across the waves, and was statistically
221 significant for the third wave (p-value = 0.037) and fourth wave (p-value = 0.022). The onset-
222 to-isolation intervals of the infectors were associated with estimated serial intervals (p-value <
223 0.005) across the waves, with shorter mean onset-to-isolation intervals correlating with shorter
224 mean serial interval estimates. Similar results were found in the sensitivity analysis for pre-
225 defined thresholds from (5-14) days (table S6).

Correction in estimation of transmissibility accounting for time-varying effective serial interval distributions

We estimated time-varying R_t to infer changes in the transmissibility of COVID-19 in Hong Kong using the Wallinga-Teunis method (*4*) (section 5, supplementary materials) which constructed the relative likelihood for a given case being a potential infector of other cases based on the case-based reproduction number (*23*). We extended the method by incorporating the effective serial interval distribution into the estimation of R_t via the *EpiEstim* package in R. The estimated R_t from time-varying effective serial intervals was compared with that based on a constant serial interval distribution over the epidemic waves.

A simulation based modelling framework was also applied to quantify the bias from using a constant over time-varying serial interval in estimating R_t through a comparison of the attack rates (or cumulative number of infections) under both approaches (section 7, supplementary materials). The time series of transmission rate β_t derived first from the R_t, estimated based on time-varying effective serial interval distributions and possible choices of constant serial interval distributions. Then these β_t were used to reconstruct the respective epidemic curves by simulating Susceptible-Infected-Recovered models to assess the related bias as the difference in attack rates from the reported data.

The differences between R_t estimated from real-time effective serial intervals and a constant serial interval distribution indicated that the latter might have introduced biases in inferring the transmissibility of COVID-19 over these 3 waves under analysis (**Fig. 3**). Smaller biases in R_t were identified during the fourth wave (except initial days) (**Fig. 3C**), during which effective serial interval distributions were relatively more stable (i.e., less varying) (**Fig. 1D**).

Furthermore, with possible choices of single constant mean (μ) and standard deviation (σ) of serial interval distributions as estimated from our data, we predicted the bias in R_t by evaluating the mean absolute deviation from the respective R_t, calculated by using effective serial intervals. The magnitude and direction (over- or under-estimate) of these biases depends on the mean as well as the standard deviation of the fixed serial interval distributions (**Fig. 3, A to C** and fig. S6). We found biases in simulated attack rates, were smaller when generated by considering the effective serial interval distributions over the respective choices of constant serial interval distributions (**Fig. 3, D to F** and table S8).

Discussion

The transmission dynamics and epidemiological characteristics of COVID-19 varied significantly over time during the earlier epidemic waves studied in Hong Kong (**Fig. 1 and Fig. 3, A to C**), accounting for changes in case profiles and the impact of various control measures implemented at that time (table S1) (*16, 17, 24*) . Our results for Hong Kong align with earlier findings for mainland China, in identifying a shortening in mean serial intervals over time as an epidemic is controlled with non-pharmaceutical interventions (*9, 11*). The first two waves in Hong Kong were notably driven by imported cases and potential super-spreading events (*17*), and the proportion of asymptomatic cases was found to be significantly higher during later waves (15% - 23%). The proportion of pre-symptomatic transmissions was up to 10%, and was significantly higher during the third wave, and comparable with the reported estimates elsewhere (*18, 25*). These inter- and intra-wave variations in case profiles along with varied PHSMs could shape the epidemiological parameters and hence the transmission dynamics of COVID-19 waves in Hong Kong.

In early 2020, we reported substantial reductions in mean effective serial intervals over time in mainland China following the implementation of various PHSMs including timely case isolation (*9*). Here we observed similar results in the second wave in Hong Kong (**Fig. 1B**), during which the mean onset-to-isolation delay had a positive association with mean serial interval and could explain a high proportion (59%) of variance in effective serial intervals. Other studies illustrated the effectiveness of the isolation of symptomatic cases and their potential contacts in achieving sustained control of COVID-19 transmission (*26, 27*). Strict isolation of cases will reduce transmission later in the infectious period (*9-11*). The measure of case isolation improved (i.e., early isolation) over time in Hong Kong (*28*) and appeared to be comparatively stable in third and fourth waves and have a lesser impact on the temporal changes in mean serial intervals (tables S3 and S4), which might have been associated with the broader application of PHSMs or demographic factors.

The community-wide PHSMs had negative association with serial interval across the waves, while case-based PHSMs, including case isolation had positive association with serial interval in the second and third wave (p-value = 0.33) (table S3). The association of these PHSMs with effective serial intervals could be positive or negative based on the impact of these interventions which could affect the infectors' infectiousness profile (as truncated or modified by case-based measures including case isolation) and effective contact pattern of infectees with potential infectors (as reduced by community-wide measures and mass testing) respectively (*9-11*) . This finding could suggest the lengthening of mean serial intervals during post-peak of third wave (during August 2020), when the per capita testing volume (as proxy of case-based measures) started to decline (fig. S7 and table S5), which might be attributable to missing of effective contact tracing and delays in isolation of cases (*29, 30*). The negative association between serial interval and community-wide PHSMs (table S3), could delay in finding

300 infectees for an infector by reducing the probability of effective contacts and resulted in reverse
301 with the strengthening of community-wide PHSMs (*30, 31*).
302
303 Along with the PHSMs, we found that certain demographic characteristics of the infectors and
304 infectees were associated with variations in serial intervals (fig. S3A and tables S7). The older
305 cases might be more severe and had faster and higher viral load (*32-39*), which might have
306 been associated with shorter latent periods and incubation periods (*36, 40-46*). Therefore, the
307 serial intervals for the transmissions from older infectors to younger infectees could be the
308 longest or vice-versa as illustrated in fig. S10. For example, we noticed from early August
309 2021, during post-peak of third wave, the mean serial interval estimates started to be longer
310 although the onset-to-isolation intervals were more or less stable (**Fig. 1C**). Although we
311 noticed on an average the infectors were older than the infectees in the transmission pairs
312 throughout the third wave and fourth waves (except during the end of fourth wave) (fig. S11).
313 Temporal variation in the age distributions of infector and infectee for a transmission chain
314 could reshape the serial interval (fig. S4). The mean infectors' age substantially increased after
315 the peak of third wave (from late June and early August 2020) and during the end of the fourth
316 wave (during February, 2021) (fig. S11), might lead longer mean serial intervals during these
317 periods (Fig. 1).
318
319 The infectors in household settings had significantly longer serial intervals for the third wave
320 in Hong Kong (fig. S3 and table S7), accounting the proportion of older infectors in household
321 was higher during that wave, though mean serial intervals under such settings reported not
322 statistically significant for the first wave in mainland China (*9, 18*). For example, the household
323 transmission was increased over time as noticed during third wave (fig. S12) and having older-
324 to-younger transmission across the course of each wave (fig. S4) might lengthen the serial

intervals during post-peak of third wave, during which mean onset-to-isolation were much stable (**Fig. 1C**).

Furthermore, the methods of estimation may affect the estimates of the serial interval distribution (*10*). Estimating temporal serial intervals via forward-looking, backward-looking or intrinsic approach by using a cohort-based framework have respective biases to be corrected (*10, 11, 47, 48*). Therefore, the estimation of reproduction number with single constant serial interval distribution can lead to bias (*9*) which can be minimised by using effective serial interval distributions instead (**Fig. 3**, fig. S6 and table S8). This bias was noticeably lower in fourth wave (**Fig. 3**) as by then the serial interval distribution had less variation across that period (**Fig. 1**).

This study provides a unique opportunity for a temporal investigation of how mean serial intervals can change over time, both shortening as well as lengthening depending on the intensity of transmission and the various case-based and community-wide PHSMs applied in Hong Kong, as well as variation in case profile (or characteristics), including demography, clinical severity, and transmission settings between and across waves. This is the first study to identify the potential factors, which could not only shorten the mean serial intervals over time, but also could lengthen the measure, therefore the resulting temporal changes in the estimates were accounted the direction and their strength of impacts. However, there are some limitations to our work. First, the change of the forward-looking serial intervals could be explained by both the PHSMs and internal mechanism (backward incubation period of infectors) (*11*), but detailed exposure information was not always available. Second, information on serial intervals collected through contact tracing could suffer various biases such as recall biases, which could reduce the chance of identifying longer serial intervals for example. However, our intense

algorithmic check and cross check with additional phylogenetic data should minimise the impact of this biases on the main outcomes. Finally, while we identified the potential for bias in R_t estimates if using constant serial interval distributions, there are other potential biases in R_t estimation that we did not discuss here.

In conclusion, our results indicated that the changes in serial interval distributions might not be always monotonic as reported earlier for mainland China in 2020 (*9*). The real-time variations in serial interval distributions were also driven by the changes in transmission pattern (who infects whom), characterised by temporal variation in demographical and clinical profiles of the cases along with PHSMs during the first two years of the COVID-19 pandemic in Hong Kong. This time varying matric of effective serial interval distributions could improve the estimation of transmissibility, the time varying reproduction number (R_t) accounting for intermediate factors of transmission and allow us to assess the timely impact of public health measures.

References and Notes

1. A. J. Kucharski *et al.*, Early dynamics of transmission and control of COVID-19: a mathematical modelling study. *Lancet Infect Dis* **20**, 553-558 (2020).
2. Y. Li *et al.*, The temporal association of introducing and lifting non-pharmaceutical interventions with the time-varying reproduction number (R) of SARS-CoV-2: a modelling study across 131 countries. *Lancet Infect Dis*, (2020).
3. A. Cori, N. M. Ferguson, C. Fraser, S. Cauchemez, A new framework and software to estimate time-varying reproduction numbers during epidemics. *Am J Epidemiol* **178**, 1505-1512 (2013).
4. J. Wallinga, P. Teunis, Different epidemic curves for severe acute respiratory syndrome reveal similar impacts of control measures. *Am J Epidemiol* **160**, 509-516 (2004).
5. C. Fraser, Estimating individual and household reproduction numbers in an emerging epidemic. *PLoS One* **2**, e758 (2007).
6. A. Svensson, A note on generation times in epidemic models. *Math Biosci* **208**, 300-311 (2007).
7. M. Lipsitch *et al.*, Transmission dynamics and control of severe acute respiratory syndrome. *Science* **300**, 1966-1970 (2003).
8. B. J. Cowling, V. J. Fang, S. Riley, J. S. Malik Peiris, G. M. Leung, Estimation of the serial interval of influenza. *Epidemiology* **20**, 344-347 (2009).
9. S. T. Ali *et al.*, Serial interval of SARS-CoV-2 was shortened over time by nonpharmaceutical interventions. *Science* **369**, 1106-1109 (2020).
10. S. T. Ali *et al.*, Serial Intervals and Case Isolation Delays for Coronavirus Disease 2019: A Systematic Review and Meta-Analysis. *Clin Infect Dis* **74**, 685-694 (2022).
11. S. W. Park *et al.*, Forward-looking serial intervals correctly link epidemic growth to reproduction numbers. *Proceedings of the National Academy of Sciences* **118**, e2011548118 (2021).
12. Centre for Health Protection (CHP) of the Department of Health, Hong Kong SAR, Latest local situation of COVID-19, (31 Decenber 2021) https://www.chp.gov.hk/files/pdf/local_situation_covid19_en.pdf. (2021).
13. B. Yang *et al.*, Changing Disparities in Coronavirus Disease 2019 (COVID-19) Burden in the Ethnically Homogeneous Population of Hong Kong Through Pandemic Waves: An Observational Study. *Clin Infect Dis* **73**, 2298-2305 (2021).
14. Y. M. Mefsin *et al.*, Epidemiology of Infections with SARS-CoV-2 Omicron BA.2 Variant, Hong Kong, January-March 2022. *Emerg Infect Dis* **28**, (2022).
15. Hong Kong Government News for COVID-19 (31 December, 2021) https://www.news.gov.hk/eng/categories/covid19/index.html). (2021).
16. P. Wu *et al.*, Suppressing COVID-19 transmission in Hong Kong: an observational study of the first four months. *09 June 2020, PREPRINT (Version 1) available at SSRN: https://papers.ssrn.com/sol3/papers.cfm?abstract_id=3627304*, (2020).
17. D. C. Adam *et al.*, Clustering and superspreading potential of SARS-CoV-2 infections in Hong Kong. *Nat Med* **26**, 1714-1719 (2020).
18. X. K. Xu *et al.*, Reconstruction of Transmission Pairs for novel Coronavirus Disease 2019 (COVID-19) in mainland China: Estimation of Super-spreading Events, Serial Interval, and Hazard of Infection. *Clin Infect Dis*, (2020).
19. D. Klinkenberg, J. A. Backer, X. Didelot, C. Colijn, J. Wallinga, Simultaneous inference of phylogenetic and transmission trees in infectious disease outbreaks. *PLoS Comput Biol* **13**, e1005495 (2017).

20. K. Leung, J. T. Wu, G. M. Leung, Real-time tracking and prediction of COVID-19 infection using digital proxies of population mobility and mixing. *Nat Commun* **12**, 1501 (2021).
21. M. U. G. Kraemer *et al.*, The effect of human mobility and control measures on the COVID-19 epidemic in China. *Science* **368**, 493-497 (2020).
22. C. O. Buckee *et al.*, Aggregated mobility data could help fight COVID-19. *Science* **368**, 145-146 (2020).
23. K. M. Gostic *et al.*, Practical considerations for measuring the effective reproductive number, Rt. *PLoS Comput Biol* **16**, e1008409 (2020).
24. B. J. Cowling *et al.*, Impact assessment of non-pharmaceutical interventions against coronavirus disease 2019 and influenza in Hong Kong: an observational study. *Lancet Public Health* **5**, e279-e288 (2020).
25. Z. Du *et al.*, Serial Interval of COVID-19 among Publicly Reported Confirmed Cases. *Emerg Infect Dis* **26**, 1341-1343 (2020).
26. Y. Ng *et al.*, Evaluation of the Effectiveness of Surveillance and Containment Measures for the First 100 Patients with COVID-19 in Singapore - January 2-February 29, 2020. *MMWR Morb Mortal Wkly Rep* **69**, 307-311 (2020).
27. A. J. Kucharski *et al.*, Effectiveness of isolation, testing, contact tracing, and physical distancing on reducing transmission of SARS-CoV-2 in different settings: a mathematical modelling study. *Lancet Infect Dis* **20**, 1151-1160 (2020).
28. H. Y. Lam *et al.*, The epidemiology of COVID-19 cases and the successful containment strategy in Hong Kong-January to May 2020. *Int J Infect Dis* **98**, 51-58 (2020).
29. B. Yang *et al.*, Universal community nucleic acid testing for COVID-19 in Hong Kong reveals insights into transmission dynamics: a cross-sectional and modelling study. *Clin Infect Dis*, (2021).
30. H. Y. Yuan, C. Blakemore, The impact of multiple non-pharmaceutical interventions on controlling COVID-19 outbreak without lockdown in Hong Kong: A modelling study. *Lancet Reg Health West Pac* **20**, 100343 (2022).
31. K. Leung, J. T. Wu, G. M. Leung, Effects of adjusting public health, travel, and social measures during the roll-out of COVID-19 vaccination: a modelling study. *Lancet Public Health* **6**, e674-e682 (2021).
32. F. Shi *et al.*, Association of viral load with serum biomakers among COVID-19 cases. *Virology* **546**, 122-126 (2020).
33. F. X. Lescure *et al.*, Clinical and virological data of the first cases of COVID-19 in Europe: a case series. *Lancet Infect Dis* **20**, 697-706 (2020).
34. Y. Liu *et al.*, Viral dynamics in mild and severe cases of COVID-19. *Lancet Infect Dis* **20**, 656-657 (2020).
35. Y. Pan, D. Zhang, P. Yang, L. L. M. Poon, Q. Wang, Viral load of SARS-CoV-2 in clinical samples. *Lancet Infect Dis* **20**, 411-412 (2020).
36. K. A. Walsh *et al.*, SARS-CoV-2 detection, viral load and infectivity over the course of an infection. *J Infect* **81**, 357-371 (2020).
37. Y. D. Gao *et al.*, Risk factors for severe and critically ill COVID-19 patients: A review. *Allergy* **76**, 428-455 (2021).
38. K. K. To *et al.*, Temporal profiles of viral load in posterior oropharyngeal saliva samples and serum antibody responses during infection by SARS-CoV-2: an observational cohort study. *Lancet Infect Dis* **20**, 565-574 (2020).
39. E. Pujadas *et al.*, SARS-CoV-2 viral load predicts COVID-19 mortality. *Lancet Respir Med* **8**, e70 (2020).

40. T. Ward, A. Johnsen, Understanding an evolving pandemic: An analysis of the clinical time delay distributions of COVID-19 in the United Kingdom. *PLoS One* **16**, e0257978 (2021).
41. M. Levine-Tiefenbrun *et al.*, Initial report of decreased SARS-CoV-2 viral load after inoculation with the BNT162b2 vaccine. *Nat Med* **27**, 790-792 (2021).
42. H. Xin *et al.*, The incubation period distribution of coronavirus disease 2019 (COVID-19): a systematic review and meta-analysis. *Clin Infect Dis*, (2021).
43. C. Leung, The difference in the incubation period of 2019 novel coronavirus (SARS-CoV-2) infection between travelers to Hubei and nontravelers: The need for a longer quarantine period. *Infect Control Hosp Epidemiol* **41**, 594-596 (2020).
44. X. He *et al.*, Temporal dynamics in viral shedding and transmissibility of COVID-19. *Nat Med* **26**, 672-675 (2020).
45. M. Levine-Tiefenbrun *et al.*, SARS-CoV-2 RT-qPCR Test Detection Rates Are Associated with Patient Age, Sex, and Time since Diagnosis. *J Mol Diagn*, (2021).
46. T. C. Jones *et al.*, Estimating infectiousness throughout SARS-CoV-2 infection course. *Science* **373**, (2021).
47. D. Champredon, J. Dushoff, Intrinsic and realized generation intervals in infectious-disease transmission. *Proc Biol Sci* **282**, 20152026 (2015).
48. S. W. Park, D. Champredon, J. S. Weitz, J. Dushoff, A practical generation-interval-based approach to inferring the strength of epidemics from their speed. *Epidemics* **27**, 12-18 (2019).
49. X. F. Liu, X. K. Xu, Y. Wu, Mobility, exposure, and epidemiological timelines of COVID-19 infections in China outside Hubei province. *Sci Data* **8**, 54 (2021).
50. S. T. Ali *et al.*, Serial intervals and case isolation delays for COVID-19: a systematic review and meta-analysis. *Clin Infect Dis*, ciab491 (2021).
51. J. T. Wu *et al.*, Nowcasting epidemics of novel pathogens: lessons from COVID-19. *Nat Med* **27**, 388-395 (2021).
52. R. Subramanian, Q. He, M. Pascual, Quantifying asymptomatic infection and transmission of COVID-19 in New York City using observed cases, serology, and testing capacity. *Proc Natl Acad Sci U S A* **118**, (2021).
53. S. T. Ali, B. J. Cowling, E. H. Y. Lau, V. J. Fang, G. M. Leung, Mitigation of Influenza B Epidemic with School Closures, Hong Kong, 2018. *Emerg Infect Dis* **24**, 2071-2073 (2018).
54. S. T. Ali *et al.*, Prediction of Upcoming Global Infection Burden of Influenza Seasons after Relaxation of Public Health and Social Measures for COVID-19 Pandemic. *Available at SSRN: https://ssrn.com/abstract=4063811 or http://dx.doi.org/10.2139/ssrn.4063811*, (2022).
55. L. Sigfrid *et al.*, What is the recovery rate and risk of long-term consequences following a diagnosis of COVID-19? A harmonised, global longitudinal observational study protocol. *BMJ Open* **11**, e043887 (2021).

Acknowledgments:

We acknowledge Ms. Julie Au for technical assistance. We thank the Centre for Health Protection in Hong Kong for their data collection and compilation throughout the COVID-19 pandemic. We thank Kathy Leung for helpful discussions. STA, DC, and acknowledge the research computing facilities and advisory services offered by Information Technology Services, The University of Hong Kong.

Funding:

Health and Medical Research Fund, Health Bureau, Government of the Hong Kong Special Administrative Region grant COVID190118 (BJC) and grant 20190712 (STA);

Collaborative Research Scheme grant C7123-20G and grant T11-705/14N, Research Grants Council, Government of the Hong Kong Special Administrative Region (BJC);

AIR@innoHK program of the Innovation and Technology Commission, Government of the Hong Kong Special Administrative Region (STA, ZD, EHYL, PW, GML, BJC);

European Research Council (grant no. 804744); the Grand Challenges ICODA pilot initiative, delivered by Health Data Research UK and funded by the Bill & Melinda Gates Foundation and the Minderoo Foundation (LW);

The funding bodies had no role in study design, data collection and analysis, preparation of the manuscript, or the decision to publish.

Author contributions:

Conceptualization: STA, PW, BJC
Methodology: STA, DC, LW, EHYL, BJC
Investigation: STA, DC, WWL, AY, DCA, YCL
Data: WWL, AY, DC, DCA, JX, FH, HG, STA
Visualization: DC, AY, YCL, STA
Comments: DCA, EHYL, LW, ZD, JYW, XKX, PW, GML, BJC
Funding acquisition: STA, EHYL, ZD, LW, PW, GML, BJC
Project administration: STA, DC, WWL, DCA, YCL
Supervision: GML, BJC

Writing – original draft: STA, DC, BJC

Writing – review & editing: STA, DCA, EHYL, LW, ZD, JYW, XKX, PW, GML, BJC

Competing interests:

BJC consults for AstraZeneca, Fosun Pharma, GSK, Moderna, Pfizer, Roche and Sanofi Pasteur. The authors report no other potential conflicts of interest.

Data and materials availability:

All data, code, and materials used in the analyses in main text and supplementary materials will be available together with the publication of this paper.

Supplementary Materials

Materials and Methods

Supplementary Text

Figs. S1 to S12

Tables S1 to S8

References (*49–55*)

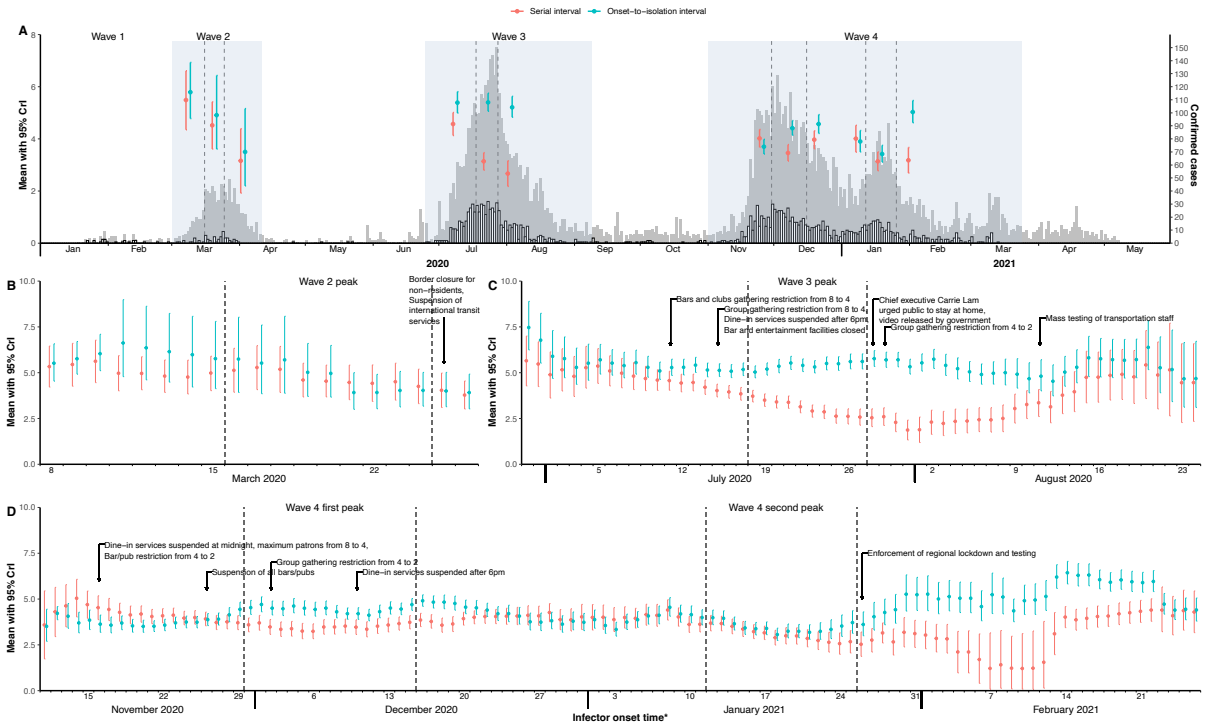

Fig. 1. Transmission dynamics and temporal estimates of serial interval distribution and isolation delay for COVID-19 in Hong Kong. (A) The grey bars indicate the epi-curve of the reported COVID-19 cases, and white bars are onset epi-curves for infectors of those reported cases during four waves in Hong Kong. Mean serial interval estimates (red dots) with 95% CrI (red vertical line segments) and mean onset-to-isolation interval (teal dots) with 95% CrI (teal vertical line segments), evaluated from all confirmed and likely transmission pairs during pre-peak, peak-timing, and post-peaks for three pre-defined waves (light blue shades) with vertical dark grey dashed lines referring to the peak-timing for each wave, with two peaks for fourth wave. (B)-(D) Time varying estimates of effective serial intervals and onset-to-isolation interval for second wave (A), third wave (B) and fourth wave (C) with the indicator to timings of major public health and social measures (PHSMs) implemented in Hong Kong. The area between two grey dashed lines in each wave indicates the peak timing of the epidemic wave. The estimates of serial interval and onset-to-isolation interval are evaluated by using MCMC on fitting normal and gamma distributions to empirical data on confirmed and likely transmission pairs (considering predefined threshold of 8 days) respectively. The effective serial intervals and onset-to-isolation intervals are estimated based on the empirical data in 10-day sliding windows (presented with respect to the 5th day of each sliding window).

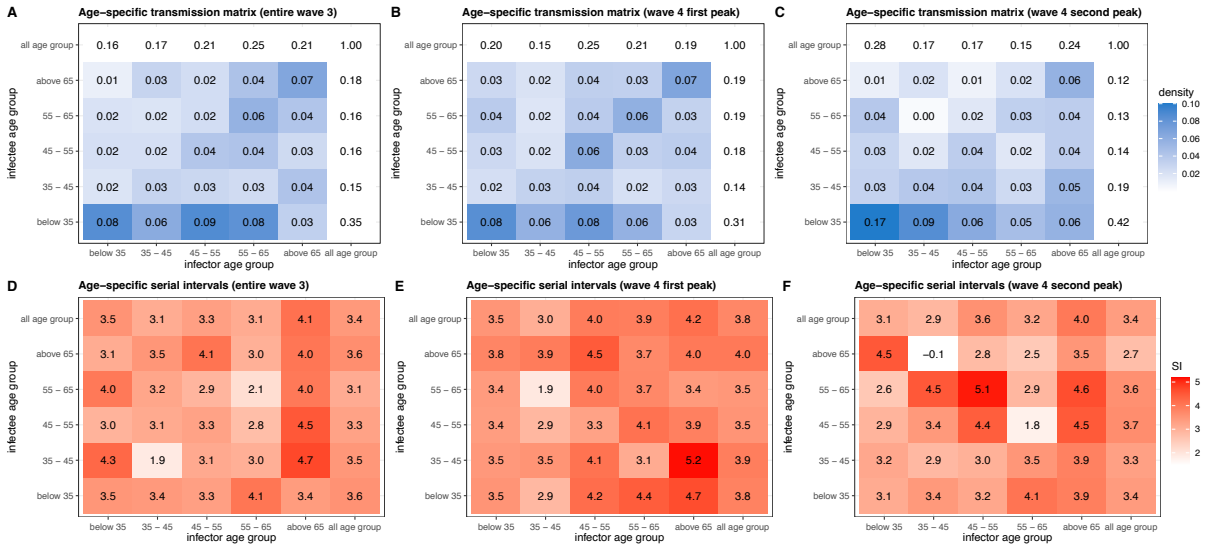

Fig. 2. Age-specific transmission and serial interval estimated between infectors and infectees for COVID-19 in Hong Kong. The heat maps for age-specific transmission densities (the relative frequency matrices of the age distribution of infector-infectee transmission pairs for the age-groups of below 35, 35-45, 45-55, 55-65, above 65 years) with the marginal densities were for third wave (A), 1st peak of fourth wave (B) and 2nd peak of fourth wave (C) of COVID-19 in Hong Kong. Age-specific empirical mean serial intervals with the respective marginal estimates, evaluated for these age-groups stratifications for infector and infectee across the third wave (D), 1st peak of fourth waves (E) and 2nd peak of fourth wave (F). Note that no infector found of age 65 years and over during second wave, hence excluded for age-specific analysis.

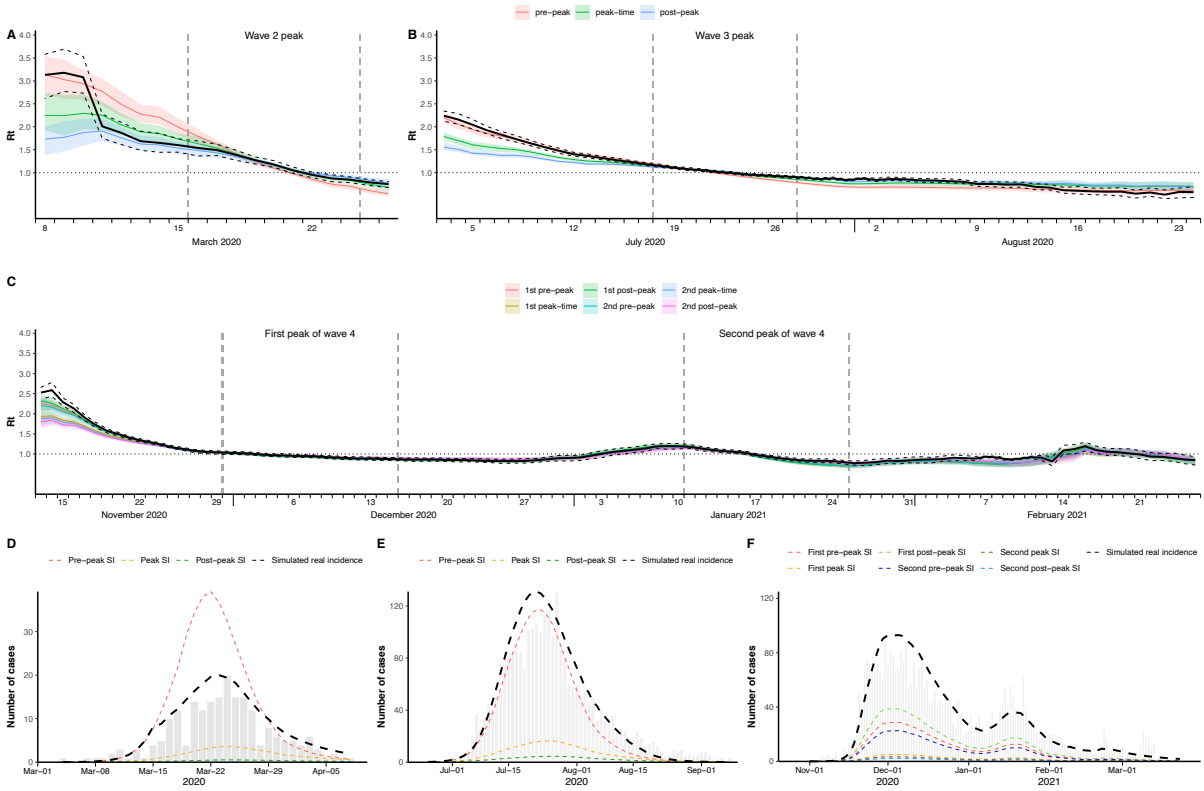

Fig. 3. Correction in transmissibility for the bias from using constant serial interval over effective serial interval distributions. Comparison of daily estimates of effective reproduction numbers (R_t) by using real-time effective serial interval distributions versus using a single fixed serial interval distributions for second wave (A), third wave (B) and fourth wave (C) in Hong Kong. The black solid lines are mean R_t (with 95% CI in dashed black lines), evaluated using effective serial interval distributions and other solid colours lines represent the mean R_t (with 95% CI in respective colours shades), evaluated using single fixed serial interval distributions. The fixed serial interval distributions with means (standard deviations) were considered for pre-, during and post-peak respectively in each wave as mean 5.5 (2.4) days, 4.5 (3.2) days and 3.2 (2.5) days for second wave; 4.6 (3.9) days, 3.1 (3.2) days and 2.7 (4.3) days for third wave; 4.0 (2.8) days, 3.5 (3.1) days and 4.0 (2.4) days for 1st peak of fourth wave; and 4.0 (3.0) days, 3.1 (2.7) days and 3.2 (3.3) days for 2nd peak of fourth wave. The differences between the black solid lines and the coloured solid lines indicate the respective biases on using single constant serial interval distribution to estimate R_t. (D)-(E) The biases in terms of attack rates, estimated by reconstructing the epi-curves via. using the transmissibility (R_t) derived by effective and constants serial interval distributions and Susceptible-Infected-Recovered (SIR) models for second wave (A), third wave (B) and fourth wave (C) in Hong Kong. The observed epi-curves (in grey bars) of the COVID-19 cases, the reconstructed epi-curves in dashed lines by using effective serial interval distributions (in black dashed lines) and different counterfactual constant serial interval distributions (in dashed coloured lines). The differences between the black dashed lines and the coloured dashed lines indicate the respective biases in attack rates on using constant serial interval distributions.